

Large Non-Stationary Noisy Covariance Matrices: A Cross-Validation Approach

Vincent W. C. Tan

Oxford-Man Institute of Quantitative Finance
Department of Engineering Science
University of Oxford
vincent.tanwengchoon@eng.ox.ac.uk

Stefan Zohren

Oxford-Man Institute of Quantitative Finance
Department of Engineering Science
University of Oxford
stefan.zohren@eng.ox.ac.uk

December 2020

Abstract

We introduce a novel covariance estimator that exploits the heteroscedastic nature of financial time series by employing exponential weighted moving averages and shrinking the in-sample eigenvalues through cross-validation. Our estimator is model-agnostic in that we make no assumptions on the distribution of the random entries of the matrix or structure of the covariance matrix. Additionally, we show how Random Matrix Theory can provide guidance for automatic tuning of the hyperparameter which characterizes the time scale for the dynamics of the estimator. By attenuating the noise from both the cross-sectional and time-series dimensions, we empirically demonstrate the superiority of our estimator over competing estimators that are based on exponentially-weighted and uniformly-weighted covariance matrices.

JEL CLASSIFICATION NOS: C13, C58, G11.

KEYWORDS: High-dimensional statistics, cross-validation, nonlinear shrinkage, exponential weighted moving average, Random Matrix Theory, rotation equivariance.

1 Introduction

The covariance matrix of asset returns is an important object for risk management and portfolio construction. In practical applications, the covariance matrix is not known *a priori* and we have to resort to estimators. When estimating a large covariance matrix, one confronts the ‘curse of dimensionality’, where the problem size grows quadratically as the number of assets increases. This means that we need to have a long enough historical dataset to produce reliable estimates of the covariances. For example, estimating a covariance matrix of 50 assets requires at least five years of daily data. The estimation of large numbers of risk parameters relative to the sample size introduces the possibility of aggregating many estimation errors from the entries of the matrix which can generate a global significant error. When such a matrix is used in the context of portfolio optimization, these errors propagate into the portfolio risk through the precision matrix.

Several estimation techniques have been proposed to overcome these issues. Structure-based estimators aim to reduce the effective number of risk parameters by incorporating prior knowledge into the estimation process such as sparsity (Bickel and Levina, 2008), graph models (Rajaratnam et al., 2008), or factor structure (Fan et al., 2012) but such regularity imposed structure may result in model biases. Linear shrinkage towards an assumed target (Ledoit and Wolf, 2004b) or a constant correlation (Ledoit and Wolf, 2004a) coefficient can offer a balance between bias and variance. These estimators, however, hinge on the assumed model or covariance matrix structure. Furthermore, they are restricted to a single common shrinkage intensity for all matrix elements, which may not be flexible enough to improve estimation in the low- and high-variance regions of the spectrum simultaneously. The eigenvalue clipping method of Bouchaud and Potters (2009) appeals to Random Matrix Theory (RMT) to describe a noise band for which all eigenvalues within it are replaced by a constant value that preserves the trace of the matrix, while maintaining the top few eigenvalues unchanged. However, this method may overestimate the eigendirections of high variance and underestimate weak factors with high Sharpe ratio (see e.g. Bartz et al., 2011; Lettau and Pelger, 2020).

Another approach is to work within the class of rotationally equivariant estimators with respect to the sample covariance due to Stein (1975, 1986), that is, estimators applicable to the Bayesian framework where we have a prior distribution on the population covariance which is equivariant under orthogonal group conjugation. Under this restriction, the best estimator of the population covariance matrix given a sample covariance matrix is one which retains the sample eigenvectors but shrinks the sample eigenvalues towards or away from their grand mean with distinct intensities by applying some nonlinear shrinkage transformation. In the high-dimensional asymptotic limit, Ledoit and P ech e (2011) showed that this transformation has a precise formula written in terms of the sample eigenvalues using the tools from RMT. A practical implementation of their formula can be achieved through discretization (Ledoit and Wolf, 2012, 2015) or kernel estimation (Ledoit and Wolf, 2020). An alternative methodology from Abadir et al. (2014), Bartz (2016) and Lam (2016) demonstrate that we can achieve a similar shrinkage effect by cross-validation where we use hold-out sets to correct for the biases in the in-sample eigenvalues. The strength of the cross-validation method is that it is model agnostic in that we make no assumptions on the distribution of the random entries of the matrix or structure of the covariance matrix.

Most of the existing covariance estimators have been developed around the sample covariance matrix, which weighs every observations equally. In the context of finance, it is well known that financial returns exhibit certain empirical regularities such as heteroscedasticity (Cont, 2001) where volatility of returns fluctuates synchronously. This volatility clustering effect can overwhelm our observations which leaves us with effectively less observations than what we originally have because the stock returns are dominated by days with large fluctuations. Thus, the use of exponentially weighted moving average covariances is relevant in non-stationary environments as it allows prior, irrelevant information to be discarded and accounts for the heteroscedasticity of volatility and correlations of financial returns. These models have been popularized in the volatility literature by RiskMetrics (J.P. Morgan/Reuters, 1996; Zumbach, 2007) for risk evaluation.

Exponential moving average covariances are attractive because they are governed by a single parameter which captures the intertemporal dependence of risks common across all the assets that require estimation. However, these matrices are also susceptible to estimation errors which are likely greater than that with uniform weights since time scale used to characterize the recent observations is smaller than the total sample size used in a typical standard sample covariance matrix. To attenuate the estimation noise in these

matrices, Pafka et al. (2004) extends the eigenvalue clipping method of Bouchaud and Potters (2009) towards exponential moving average covariances. By contrast, the Dynamic Conditional Correlation (DCC) model proposed by Engle (2002), is another popular approach to model conditional heteroscedasticity. The DCC also suffers from the ‘curse of dimensionality’ as number parameters to be estimated in the DCC increases with the dimensionality of the problem size. There have been efforts from Engle et al. (2019) to successfully enable the estimation of the DCC to be both computationally feasible in the high-dimensional setting through composite likelihood functions and with reduced estimation error through nonlinear shrinkage.

Our view is that maintaining a single parameter as in the exponential moving average covariances can offer a more parsimonious representation of asset returns than the DCC, which also enable us to study its spectral properties with a few high level bulk variables. In this paper, we introduce a covariance matrix estimator that extends the cross validation procedure of Bartz (2016) towards exponential moving average covariances. By recognizing that these matrices belong to a general class of weighted estimators of the population covariances, which themselves can be interpreted as a standard sample covariance matrix expressed in a different basis (Burda et al., 2011), we can operationalize the cross-validation computations across the weighted data examples. We show that our proposed method can reduce the excess dispersion of the sample eigenvalues which are inflated along two dimensions; that is, the cross-section and time-series dimensions due to high-dimensional and non-stationary noise, respectively.

Furthermore, while the use of exponential moving average covariances is appropriate for capturing non-stationary nature of financial returns, the price that we have to pay for such added flexibility is the requirement to tune a hyperparameter, the exponential decay parameter. We show phenomenologically, and illustrate by our experiments that RMT can be helpful in providing us guidance in choosing a suitable hyperparameter which, in machine learning parlance, we interpret as a regularization parameter that prevents the covariance matrix from overfitting to the recent observations. We demonstrate through empirical examples on liquid stock returns from the CRSP dataset that our estimator outperforms competing estimators based on uniformly- and exponentially-weighted covariance matrices.

The paper is structured as follows. Section 2 reviews the rotational equivariant covariance matrix estimators. Section 3 defines the exponential moving average covariance matrix, motivates for the need of shrinking their sample eigenvalues, and describes of our cross-validation estimator and approach for hyperparameter tuning. Section 4 contains Monte Carlo simulations. Section 5 provides the empirical experiments. Section 6 concludes.

2 Background

2.1 Rotational Equivariant Estimator

Let $\mathbf{X} = (\mathbf{x}_1, \dots, \mathbf{x}_T)'$ be a $T \times N$ matrix of T independent observations of the sample vector, \mathbf{x}_t , each of dimensionality N . Here, \mathbf{X}' denotes the transpose of \mathbf{X} . The sample vector is assumed to have zero mean and have a population covariance matrix \mathbf{C} which is not known *a priori*. The sample covariance matrix (SCM) is defined as

$$\hat{\mathbf{S}} := \frac{1}{T} \mathbf{X}' \mathbf{X}. \quad (1)$$

The SCM is an estimator of \mathbf{C} since it is unbiased; in other words, $\mathbb{E}[\hat{\mathbf{S}}] = \mathbf{C}$. It is also consistent under standard asymptotics where the matrix dimension N is fixed. However, when the dimensionality of the problem is of the same order as the sample size, it is well known that the SCM can become ill-conditioned and perform poorly out-of-sample. Consider the eigendecomposition of the SCM given by $\hat{\mathbf{U}}' \hat{\mathbf{\Gamma}} \hat{\mathbf{U}}$ where $\hat{\mathbf{\Gamma}}$ is a diagonal matrix consisting of the sample eigenvalues $\hat{\gamma} := (\hat{\gamma}_1, \dots, \hat{\gamma}_N)$ with corresponding rotation matrix $\hat{\mathbf{U}}$ whose i th column vector is the i th sample eigenvector $\hat{\mathbf{u}}_i$. Since the eigenvectors are orthogonal by construction, it is always well-conditioned, and hence, leaving the source of ill-conditioning to the eigenvalues.

In general, the problem of developing a covariance estimator that is better conditioned than the SCM is intractable because one has to estimate a matrix with $O(N^2)$ elements from a noisy matrix with identical

dimensionality. Thus, in order to reduce the degrees of freedom from $O(N^2)$ to $O(N)$, we work within the class of *rotational equivariance* estimators due to [Stein \(1975, 1986\)](#).

Let $\hat{\Sigma} \equiv \hat{\Sigma}(\hat{\mathbf{S}})$ be a covariance estimator of \mathbf{C} . An estimator is said to be rotational equivariant if $\hat{\Sigma}(\mathbf{R}\hat{\mathbf{S}}\mathbf{R}) = \mathbf{R}\hat{\Sigma}(\hat{\mathbf{S}})\mathbf{R}$ for any N -dimensional rotation matrix \mathbf{R} . These class of estimators are agnostic to the direction of the largest or smallest risk, that is, it is an isotropy hypothesis of equal probabilities for all direction. One can show that this leads to estimators that have the same eigenvectors as the SCM, which has the following form

$$\Sigma(\hat{\mathbf{S}}) = \sum_{i=1}^N \xi_i \hat{\mathbf{u}}_i \hat{\mathbf{u}}_i',$$

where $\boldsymbol{\xi} := (\xi_1, \dots, \xi_N)$ is the N -dimensional vector that is needed to be estimated. Given a SCM, the optimal corrected eigenvalues are given by $\boldsymbol{\xi}^* := (\xi_1^*, \dots, \xi_N^*)$ through the following minimization problem

$$\boldsymbol{\xi}^* = \arg \min_{\boldsymbol{\xi}} \left\| \mathbf{C} - \sum_{i=1}^N \xi_i \hat{\mathbf{u}}_i \hat{\mathbf{u}}_i' \right\|_{\text{F}}^2, \quad (2)$$

where $\|\mathbf{A}\|_{\text{F}}^2 = \text{Tr}(\mathbf{A}\mathbf{A}')$ is the Frobenius matrix norm. The solution to this optimization problem is given by the following expression

$$\xi_i^* = \hat{\mathbf{u}}_i' \mathbf{C} \hat{\mathbf{u}}_i = \sum_{j=1}^N (\hat{\mathbf{u}}_i' \mathbf{u}_j)^2 \gamma_j, \quad \text{for } i = 1, \dots, N, \quad (3)$$

where \mathbf{u}_j is the j th population eigenvector associated with the j th population eigenvalue γ_j . From Equation (3), we see that if the sample eigenvectors coincide with the population eigenvectors, then $\{\xi_i^*\}_{i=1}^N$ are the population eigenvalue. However, if there are deviations of the sample eigenvectors from their population counterparts, then the population eigenvalues are no longer optimal with respect to the Frobenius norm. This is because ξ_i^* takes into account the fact that the sample eigenvectors are not the population eigenvectors; it optimally adjusts in such a way that it minimizes the estimation error of the sample eigenvectors. In fact, in [Ledoit and Wolf \(2004b\)](#) it is shown that $\{\xi_i^*\}_{i=1}^N$ are less dispersed than the sample eigenvalues $\{\hat{\gamma}_i\}_{i=1}^N$.

We can use Equation (3) to arrive at the so-called finite-observation optimal estimator (FSOPT) defined in [Ledoit and Wolf \(2020\)](#) as

$$\Sigma^*(\hat{\mathbf{S}}) := \sum_{i=1}^N \xi_i^* \hat{\mathbf{u}}_i \hat{\mathbf{u}}_i'.$$

Note that the reconstructed covariance matrix Σ^* is a positive-definite matrix provided the population eigenvalues and the squared overlaps between the sample and population eigenvectors are greater than zero. The FSOPT is a general purpose estimator that does not assume any *a priori* information on the eigenvectors of the population covariance matrix; it only adjusts the sample eigenvalues such that it has minimum Frobenius error among the matrices that share the same eigenvectors as the SCM.

2.2 Spectrum Correction Estimators

The optimal finite observation result of $\Sigma^*(\hat{\mathbf{S}})$ with respect to the $\hat{\mathbf{S}}$ is not feasible in practice as it requires the knowledge of $\boldsymbol{\xi}^*$ which depends on the unobservable population covariance matrix \mathbf{C} . There are two existing approaches that aims to make the FSOPT amenable to estimation: (non-)linear shrinkage and cross-validation. In the former approach, the first-generation technology was the linear shrinkage estimator of [Ledoit and Wolf \(2004b\)](#) which takes the convex combination between the sample covariance matrix and the identity matrix in order to produce a composite matrix that is a low-variance high-bias estimator of the covariance. In effect, it shrinks the sample eigenvalues towards their grand mean according to

$$\hat{\xi}_i^{\text{ls}} \equiv \hat{\xi}^{\text{ls}}(\hat{\gamma}_i) = \rho \hat{\gamma}_i + (1 - \rho) \bar{\gamma}, \quad \text{for } i = 1, 2, \dots, N, \quad (4)$$

where $\rho \in [0, 1]$ is the shrinkage intensity and with $\bar{\gamma}$ denoting the average of the eigenvalues of the SCM. The attractiveness of linear shrinkage lies in the fact that it only uses $O(1)$ degrees of freedom, and there is a fast and numerically robust method provided by [Ledoit and Wolf \(2004b\)](#) to estimate the optimal shrinkage intensity. This estimator belongs to the rotation equivariance class but can be asymptotically suboptimal.

A nonlinear generalization of linear shrinkage appeals to the high-dimensional asymptotic limit where matrix dimension N and sample size T tend to infinity with the ratio N/T converging to a fixed limit $q \in (0, 1)$. Under this double asymptotic regime, the Random Matrix Theory (RMT) framework developed by [Wigner \(1955\)](#) in the context of nuclear physics is used to relate the limiting sample and population spectral distributions. In particular, such relationship can be described through [Marčenko and Pastur \(1967\)](#) law. In many research problems in RMT, the distribution of the sample eigenvalues is inferred from the distribution of the population eigenvalues in order to make phenomenological predictions. Conversely, in covariance matrix estimation, the inverse of this inference problem takes precedence; this involves recovering the population eigenvalues from a given set of sample eigenvalues through the inversion of the Marčenko-Pastur law (see e.g. [El Karoui, 2008](#); [Ledoit and Pécché, 2011](#)).

The seminal work of [Ledoit and Pécché \(2011\)](#) operates under the rotational equivariance restriction and the high-dimensional asymptotic limit which showed that there is a formula which approximates the optimal finite-observation shrinkage expression in Equation (3) and does not depend on the population covariance matrix. The formula is given by the following expression

$$\xi_i^{\text{nl}} \equiv \xi^{\text{nl}}(\hat{\gamma}_i) = \frac{\hat{\gamma}_i}{|1 - q - q\hat{\gamma}_i G_{\mathbf{S}}(\hat{\gamma}_i)|^2}, \quad \text{for } i = 1, 2, \dots, N, \quad (5)$$

where q is the (limiting) concentration ratio, and $G_{\mathbf{S}}(z)$ is the Stieltjes transform of the continuous spectral density of the sample eigenvalues of the SCM.¹ It is a nonlinear function where each sample eigenvalues $\hat{\gamma}_i$ is adjusted by a correction factor whose influence intensifies at higher concentrations where the sample size is comparable to the number of variables. Unlike the linear shrinkage which is a global operator that pulls all the sample eigenvalues towards the same common center of mass, the nonlinear shrinkage is a local operator which attracts samples eigenvalues toward the center of mass closest to it ([Ledoit and Wolf, 2020](#)).

An asymptotically optimal *bona fide* version of Equation (5) that only depends on observable quantities was developed by [Ledoit and Wolf \(2012\)](#); we denote it as $\{\hat{\xi}_i^{\text{nl}}\}_{i=1}^N$. This requires the estimation of an integral transform for $G_{\mathbf{S}}(z)$ from discrete observed data which relies on the Marčenko-Pastur law. To address this problem, [Ledoit and Wolf \(2012, 2015\)](#) discretizes the Marčenko-Pastur law to obtain the relationship between the discrete sample eigenvalues to its population counterparts using a deterministic multivariate function called Quantized Eigenvalues Sampling Transform (QuEST). A numerical inversion of the QuEST function provides an estimate for the population eigenvalues, which allows the computation of the complex-valued function $\hat{G}_{\mathbf{S}}(z)$. Alternatively, [Ledoit and Wolf \(2020\)](#) estimate the limiting density of the SCM through the use of nonparametric kernels to compute Stieltjes transform from discrete data.

A different approach which optimizes the same loss function as that of nonlinear shrinkage in Equation (2) but does not make any assumption on the structure of the noise on the entries of the matrix is through the validation procedure utilized in [Bartz \(2016\)](#). In particular, the K -fold cross-validation (CV) estimator for the sample eigenvalues of the SCM that approximates Equation (3) is given by

$$\hat{\xi}_i^{\text{cv}} := \frac{1}{K} \sum_{k=1}^K \sum_{t \in \mathcal{I}_k} \frac{1}{|\mathcal{I}_k|} (\hat{\mathbf{u}}_i[k]' \mathbf{x}_t)^2, \quad \text{for } i = 1, 2, \dots, N, \quad (6)$$

where $\hat{\mathbf{u}}_i[k]$ is the i th sample eigenvector associated to the i th eigenvalue of the SCM in which we discard all the observations belonging to the set \mathcal{I}_k for a fixed $k = \{1, 2, \dots, K\}$, and \mathbf{x}_t is the sample vector belonging to the set \mathcal{I}_k . This estimator uses an independent dataset as a proxy for the population covariance matrix to correct for the biases from the in-sample eigenvalues. Moreover, [Lam \(2016\)](#) showed that $\{\hat{\xi}_i^{\text{cv}}\}_{i=1}^N$ is positive almost surely provided the population covariance matrix \mathbf{C} is positive-definite.

¹See Appendix A.1 for the definition of the Stieltjes transform.

When $K = 1$, the CV estimator coincides with that of leave-one-out cross-validation (LOOCV). However, [Bartz \(2016\)](#) demonstrated that LOOCV can suffer from high estimation error due to the noisy nature of the rank-one matrices from the hold-out set. Thus, the use of moderately sized hold-out set of size $K > 1$ along with averaging over the folds, can further attenuate noise in the estimated eigenvalues. As a by-product of using a larger sized hold-out set, the computational cost of implementing the K -fold estimator is also reduced considerably since it employs fewer eigendecompositions of many different high-dimensional matrices.

3 Proposed Methodology

3.1 Problem Set-Up

To address the problem of heteroscedasticity in the time-series setting, we consider a sample covariance matrix that is measured using an exponential weighted moving average weighting scheme, henceforth, EMA-SCM,

$$\hat{\mathbf{E}} \equiv \hat{\mathbf{E}}(\tau, T) := \frac{1 - \beta}{1 - \beta^T} \sum_{t=1}^T \beta^{t-1} \mathbf{x}_{\tau-t-1} \mathbf{x}'_{\tau-t-1}, \quad (7)$$

where τ is the last calendar date in the estimation window of length T , and $\beta \in (0, 1)$ is the exponential decay rate. Note that the exponential weights are normalized so that their sum equals to one. Intuitively, the EMA-SCM places more weight on recent observations by discounting old data in an exponential fashion. Alternatively, the EMA-SCM can be expressed through a recurrence relation given by

$$\hat{\mathbf{E}}(\tau, T) = \beta \hat{\mathbf{E}}(\tau - 1, T - 1) + (1 - \beta) \mathbf{x}_\tau \mathbf{x}'_\tau, \quad (8)$$

where the weights $1 - \beta$ and β reflect the sensitivity to the recent rank-one return cross-products, and the average of the historical rank-one covariances, respectively. Both expressions in Equation (7) and (8) coincide when the dependence on the initial covariance matrix, $\hat{\mathbf{E}}(\tau, 0)$ is removed by setting it to zero.

The time frame for which the observations are “effectively” measured can be determined using a characteristic time-scale defined as $T_e := -1/\log(\beta)$. In practice, the decay rate is often chosen such that the characteristic time-scale is smaller than the sample size. This, however, introduces an additional channel for which estimation errors could propagate into the system since we are now measuring the observations with a sample size that is effectively smaller to describe the same high-dimensional system. Indeed, from Equation (8), we see that the hyperparameter β describes the intertemporal dependence of risk between two time periods τ and $\tau - 1$. A higher sensitivity of the EMA-SCM to the recent return allows a more reactive estimator towards information from the recent past but at the cost of introducing recent noisy observations into the estimation process. We shall analyze this phenomena in further detail in Section 3.3.

It is instructive to define the effective concentration ratio $N(1 - \beta)$ which we regard as an effective measure for the curse of dimensionality. As we are interested in the high-dimensional asymptotic limit, we assume that the regular and effective concentration ratios converge to their respective fixed limit; that is, $N/T \rightarrow q \in (0, 1)$ and $N(1 - \beta) \rightarrow q_e \in (0, 1)$ as $N, T \rightarrow \infty$ and β tends to 1 (from below). Furthermore, we use the approximation of the characteristic time-scale where $T_e \sim (1 - \beta)^{-1} \sim -1/\ln(\beta)$ under this limit.

3.2 Weighted Covariance Estimator

In general, the standard SCM can be extended by considering the weighted covariance matrix of the following form

$$\hat{\mathbf{E}} = \frac{1}{T} \mathbf{X}' \mathbf{B} \mathbf{X}, \quad (9)$$

where \mathbf{B} is a fixed symmetric and positive-definite $T \times T$ matrix such that $T^{-1} \text{Tr}(\mathbf{B})$ tends to a constant as $T \rightarrow \infty$. Without loss of generality, we assume that $T^{-1} \text{Tr}(\mathbf{B}) = 1$. These weighted covariance matrices are

also unbiased estimators of \mathbf{C} since

$$\mathbb{E}[\hat{\mathbf{E}}] = \frac{1}{T} \mathbb{E}[\mathbf{X}'\mathbf{B}\mathbf{X}] = \mathbf{C}.$$

If \mathbf{B} is chosen to be a diagonal matrix with the following weight profiles

$$[\mathbf{B}]_{tt'} := T \frac{1-\beta}{1-\beta^T} \beta^{t-1} \delta(t-t'), \quad \text{for } t = 1, 2, \dots, T,$$

where $\delta(\cdot)$ is the Dirac delta function centered at 0, then we arrive at the expression for the EMA-SCM. Further, making the following change of variables

$$\tilde{\mathbf{X}} \equiv \tilde{\mathbf{X}}(\beta) := \mathbf{X}\mathbf{B}^{1/2}, \quad (10)$$

renders $\hat{\mathbf{E}}$ to be of the similar form as the SCM. By making a specific modification to the matrix \mathbf{X} using matrix \mathbf{B} , we implicitly incorporate prior information about the data; in our case, it is the non-stationarity of financial returns. As such, $\hat{\mathbf{E}}$ in the EMA-SCM formalism has a different eigenbasis to $\hat{\mathbf{S}}$ in the SCM formalism; we write the eigendecomposition $\hat{\mathbf{E}} = \hat{\mathbf{V}}'\hat{\mathbf{\Lambda}}\hat{\mathbf{V}}$ where $\hat{\mathbf{\Lambda}}$ is a diagonal matrix consisting of the sample eigenvalues $\hat{\boldsymbol{\lambda}} := (\hat{\lambda}_1, \dots, \hat{\lambda}_N)$ with corresponding matrix of eigenvectors $\hat{\mathbf{V}}$ whose i th column vector of is the i th sample eigenvector $\hat{\mathbf{v}}_i$.

When \mathbf{B} is a positive-definite matrix, the weighted covariance matrix can be interpreted as a standard SCM under correlated sampling (Burda et al., 2011). Indeed, we see that the weights from the EMA-SCM in Equation (9) induce correlations into an otherwise uncorrelated series of the form

$$\mathbb{E}[\tilde{x}_{ti}\tilde{x}_{ti'}] = \frac{1-\beta}{1-\beta^T} \beta^{t-1} \delta(t-t'), \quad (11)$$

for $t = 1, 2, \dots, T$ and $i = 1, \dots, N$. As a result, the variance of the weighted random variables \tilde{x}_{ti} now have a time dependent structure, which decays geometrically over time.

3.3 Spectrum of Exponential Weighted Moving Average Covariances

To understand the effect of noise on $\hat{\mathbf{E}}$ in the EMA-SCM formalism, we analyze how both the (limiting) concentration ratio q and effective concentration ratio q_e affect a large complex system of asset returns by treating the observations in the original matrix \mathbf{X} is a matrix of independent and identically distributed (i.i.d.) standard normal random variables of dimension $T \times N$. This treatment can give us insights into bulk behavior of a large system, which can be described through a finitely supported limiting spectral distribution (LSD) of $\hat{\mathbf{E}}$, denoted as $\rho_{\mathbf{E}}(\lambda; q, q_e)$. There have been several works dedicated to analytically deriving the LSD of the EMA-SCM; (see e.g. Bouchaud and Potters, 2009, 2020; Bouchaud et al., 2005; Burda et al., 2011; Pafka et al., 2004); we provide a derivation of this LSD, using free probability theory in Appendix A.3.

The left panel of Figure 1 plots $\rho_{\mathbf{E}}(\lambda; 0.5, q_e)$ for different values of the effective concentration ratio q_e with a fixed concentration ratio at $q = 0.5$. In the limiting case where $q_e = 0$, the LSD of $\hat{\mathbf{E}}$ converges to the Marčenko and Pastur (1967) density, which describes the asymptotic average density of eigenvalues of a Wishart matrix $\mathbf{X}'\mathbf{X}/T$. The Marčenko-Pastur density, denoted as ρ_{MP} , has an analytical expression given by

$$\rho_{\mathbf{E}}(\lambda; q, 0) \equiv \rho_{\text{MP}}(\lambda; q) := \begin{cases} f(\lambda) & \text{if } \rho < 1 \\ (1-q^{-1})\delta(\lambda) + f(\lambda) & \text{otherwise} \end{cases},$$

where $\delta(\lambda)$ is a Dirac delta density located at 0, and f is a density function of the following form

$$f(\lambda) = \frac{1}{2\pi\lambda q} \sqrt{(\lambda - \lambda_-)(\lambda_+ - \lambda)}.$$

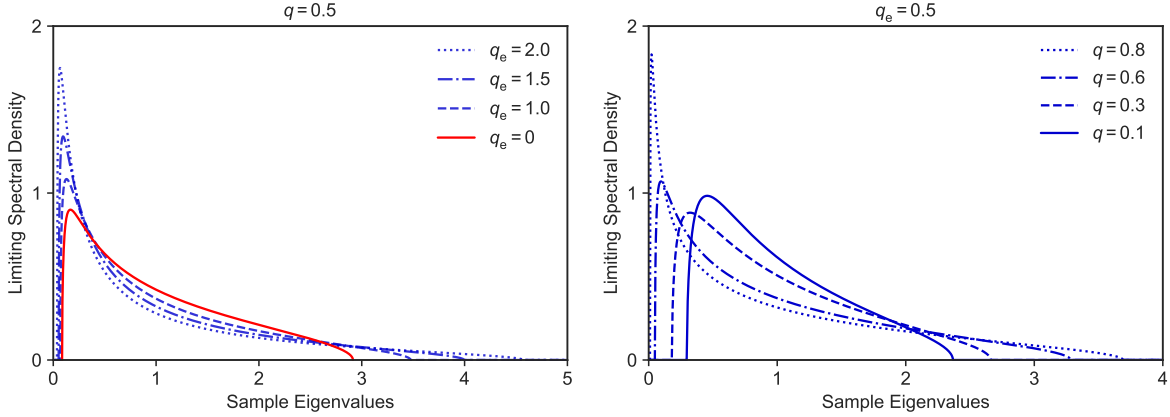


Figure 1: The limiting spectral density of sample eigenvalues for the EMA random matrix when the population covariance matrix is equal to the identity matrix for various effective concentration levels (left panel) concentration levels (right panel). When q_e tends to zero for a fixed $q > 0$, the limiting spectral density tends to the Marčenko and Pastur density with concentration level q .

for λ within a compact support defined by the upper and lower edges $\lambda_{\pm} = (1 \pm \sqrt{q})^2$. When the number of observations is comparable to the dimensionality of the system with $q = 0.5$, the Marčenko-Pastur distribution $\rho_{\text{MP}}(\lambda; 0.5)$ exemplifies that the sample eigenvalues are dispersed around their mean centered at one; the smallest (largest) sample eigenvalues are biased downwards (upwards) by random sampling. The Marčenko-Pastur distribution can be regarded as a “null model” and that excess dispersion here is driven by the high-dimensional noise in the cross-section.

The excess dispersion of $\rho_{\mathbf{E}}(\lambda; 0.5, q_e)$, however, becomes larger when effective concentration q_e increases even if the concentration ratio is held fixed at $q = 0.5$. In particular, the LSD becomes more right-skewed than the Marčenko-Pastur distribution; there is a larger concentration of the mass of the LSD near the zero eigenvalue and a wider spread of the support. This is because the variance of the weighted random variables \tilde{x}_{ti} now has a time dependent structure. The lower edge of the LSD also decays exponentially fast towards zero (see Appendix A.3). As a result, the LSD of the EMA-SCM deviates from the Marčenko-Pastur distribution which reflects a contamination of isotropic noise profile due to the non-stationarity of the sample covariances in time.

Finally, the right panel of Figure 1 shows how different concentration ratios affect the LSD $\rho_{\mathbf{E}}(\lambda; q, 0.5)$ while maintaining the effective concentration at $q_e = 0.5$. We see that higher concentrations systematically inflates the excess dispersion as expected. However, the marginal increment in excess dispersion from varying q can be attributed to the noise from the cross-sectional dimension since the decay rate is held constant. This analysis suggests that the systematic bias arising from both the cross-sectional and time-series dimensions must be corrected by shrinking the distribution of sample eigenvalues towards the center.

3.4 Cross-Validation Shrinkage Estimator

In light of the previous discussion, we introduce covariance estimator that corrects for the biases in the sample eigenvalues of the EMA-SCM. We extend the estimator of Bartz (2016) stated in Equation (6) and define our K -fold cross-validation estimator for the eigenvalues of the matrix $\hat{\mathbf{E}}$ in the EMA-CV formalism as

$$\hat{\xi}_i^{\text{cv}}(\beta) := \frac{1}{K} \sum_{k=1}^K \sum_{t \in \mathcal{I}_k} \frac{1}{|\mathcal{I}_k|} (\hat{\mathbf{v}}_i[k]' \tilde{\mathbf{x}}_t)^2, \quad \text{for } i = 1, 2, \dots, N, \quad (12)$$

where $\hat{\mathbf{v}}_i[k]$ is the i th sample eigenvector of the $\hat{\mathbf{E}}$ in which all the observations from the set \mathcal{I}_k for a fixed $k = \{1, 2, \dots, K\}$ are discarded, and $\tilde{\mathbf{x}}_t$ is the sample vector from matrix $\tilde{\mathbf{X}}$ defined in Equation (10) belonging

to the set \mathcal{I}_k . In all of our simulation and empirical experiments, we choose the number of folds K to be 10 to obtain a reliable estimate of the optimal finite sample corrected eigenvalues given in Equation (3) with reduced computational overhead from the brute-force eigendecompositions.

A benefit introducing the auxiliary variables $\tilde{\mathbf{X}}$ is that it allows us to represent $\hat{\mathbf{E}}$ in the same form as the SCM in Equation (1) by disentangling the time dependence structure shared across the observations. This is possible due to the deterministic and diagonal structure of the weight matrix \mathbf{B} . Thus, we can partition the observation matrix $\tilde{\mathbf{X}}$ into two subsamples, a training fold and a test fold, and operationalize the cross-validation procedure of Bartz (2016) towards the EMA-SCM.

Note that CV requires that the data in the training and test folds to be independent so that the projection of the eigenvector onto the data can be expected to be less adversely impacted by noise when estimating the eigenvalues. Since the moving average weights induces autocorrelation into an otherwise uncorrelated series, we shuffle the entire auxiliary data before splitting into folds to break the temporal correlations of the series so that the folds based on consecutive data points can be approximately independent.

Since the sample vector \mathbf{x}_t is independent of $\hat{\mathbf{v}}_i[k]$ with $\mathbb{E}[\mathbf{x}_t \mathbf{x}_t'] = \mathbf{C}$, and exponential weights sum to one, we have

$$\mathbb{E}[\hat{\xi}_i^{\text{cv}}(\beta)] = \frac{1}{K} \sum_{k=1}^K \sum_{t \in \mathcal{I}_k} \frac{1}{|\mathcal{I}_k|} \mathbb{E}[(\hat{\mathbf{v}}_i[k]' \tilde{\mathbf{x}}_t)^2] = \mathbb{E}[\hat{\mathbf{v}}_i[k]' \mathbf{C} \hat{\mathbf{v}}_i[k]].$$

Additionally, we perform an isotonic regression (Barlow et al., 1972) of the set cross-validated eigenvalues $\{\hat{\xi}_i^{\text{cv}}(\beta)\}_{i=1}^N$ on the sample eigenvalues of $\hat{\mathbf{E}}$ to enforce a monotonic structure on the sequence of bias-corrected eigenvalues which we denote as $\hat{\xi}_i^{\text{iso-cv}}(\beta) \equiv \hat{\xi}_i^{\text{iso-cv}}(\hat{\lambda}_i; \beta)$ for $i = 1, 2, \dots, N$.

Since we are working within the class of rotation equivariant estimators, we reconstruct the new covariance matrix using the estimated eigenvalues with the eigenvectors from the original EMA-SCM

$$\hat{\Sigma}(\hat{\mathbf{E}}; \beta) = \sum_{i=1}^N \hat{\xi}_i^{\text{iso-cv}}(\hat{\lambda}_i; \beta) \hat{\mathbf{v}}_i \hat{\mathbf{v}}_i'.$$

The covariance $\hat{\Sigma}(\hat{\mathbf{E}}; \beta)$ is parameterized by β due to its dependence on the EMA-SCM. An estimate for the inverse covariance is then obtained by the inverse of the covariance estimator.

3.5 Calibrating the Limiting Spectral Density to Data

While our proposed EMA-CV method is suitable for controlling the noise in the cross-sectional dimension, it introduces an additional channel for which noise can permeate into the estimation process; that is, through the time-series dimension. A way to reduce overfitting to the recent observations is through regularization in the time-series dimension, which can be achieved by inducing further memory of historical observations into the EMA-SCM through the exponential decay rate, β .

For our empirical applications, we argue that it is possible to choose the parameter β without the need to infer future performance from out-of-sample data. This is possible from the self-averaging property of large matrices in RMT, where one observation is usually sufficient to provide us information about the distribution (Bun et al., 2017).² Since we can get the prior from the data, it is appropriate to calibrate the LSD $\rho_{\mathbf{E}}(\lambda; q, q_e)$ to the bulk of sample spectral density (SSD) from the SCM through q_e . While this implicitly amounts to assuming that the data generating process is random, it can serve as a minimal model to describe the highly complex disordered nature of high-dimensional financial returns.

To perform such calibration for the decay rate β , we propose to fit the LSD $\rho_{\mathbf{E}}(\lambda; q, q_e)$ to the SSD, denoted as $\hat{\rho}_N(\lambda; p)$, where p is the number of outliers that we wish to remove from the SSD. In particular, we remove p outliers from the SSD reduces its skewness and use a kernel density to smooth out the random variation of the SSD. Both of these processing efforts help facilitate a more accurate calibration of the LSD

²Note that this statement is not true in general for Bayesian theory as we usually need to inject a prior. However, in the high-dimensional asymptotic limit and assuming rotational equivariance, we can build our own prior from the data.

to the bulk of the SSD. We write the continuous density of the sample eigenvalues according to the following construction

$$\hat{\rho}_{\mathbf{S}}(\lambda; p, h) := \frac{1}{N} \sum_{i=1}^N K_h(\lambda - \hat{\lambda}_i; p),$$

where K is the kernel and $h > 0$ is the bandwidth parameter that controls the degree of smoothing. We will consider the Gaussian kernel for $K_h(\cdot)$ for our experiments. We then search for the optimal effective concentration ratio q_e such that the distance between the two continuous spectral densities is minimized. Together with an appropriately chosen bandwidth parameter and number of outliers removal, the optimization problem can be formulated as

$$\hat{q}_e = \arg \min_{q_e} \mathbb{D}(\hat{\rho}_{\mathbf{S}}(\lambda; \hat{p}, \hat{h}), \rho_{\mathbf{E}}(\lambda; q_e)), \quad (13)$$

where \mathbb{D} is a distance measure between two spectral distributions. To define a divergence metric between the spectral measures, we consider the Jensen-Shannon divergence (Lin, 1991) which is a symmetrized version of Kullback-Leibler divergence.

4 Monte Carlo Simulations

4.1 Simulation Design

To test the validity of our proposed estimator in the cross-sectional dimension, we perform Monte Carlo simulations following Ledoit and Wolf (2012), which considers independent and identically distributed (i.i.d.), normal random variables with population eigenvalues set to be 20%, 40% and 40% of the eigenvalues to 1, 3 and 10, respectively. A feature of this design is that when the concentration ratio is 1/3 or smaller, the standard SCM exhibits a ‘‘spectral separation’’ where the sample eigenvalues are clustered into a Dirac of population eigenvalue. However, differently from the experimental context around the standard SCM in Ledoit and Wolf (2012), this spectral separation pattern becomes further obscured when we consider the EMA-SCM since the observations are now weighted across time. As such, this provides an additional hurdle for covariance matrix estimators to correct the eigenvalues appropriately.

We consider post-processing the EMA-SCM with linear shrinkage (Ledoit and Wolf, 2004b) and nonlinear shrinkage (Ledoit and Wolf, 2020), which we denote as EMA-LS and EMA-NL, respectively. While these two methods were originally developed for the standard SCM, they provide an interesting benchmark for us to gain an insight into their behavior when they are applied towards the EMA-SCM, and to determine whether there are gains to be realized from our proposed method. The covariance estimators $\hat{\Sigma}$ are compared using the performance measure SEPRIAL (eigenbasis percentage improvement in average loss) with respect to the EMA-SCM which is given by

$$\text{SEPRIAL}(\hat{\Sigma}(\hat{\mathbf{E}}; \beta)) := \left(1 - \frac{\mathbb{E} \|\hat{\Sigma}(\hat{\mathbf{E}}; \beta) - \Sigma(\hat{\mathbf{E}}; \beta)\|^2}{\mathbb{E} \|\hat{\mathbf{E}}(\beta) - \Sigma(\hat{\mathbf{E}}; \beta)\|^2} \right) \times 100\%,$$

where $\Sigma(\hat{\mathbf{E}}; \beta)$ is the FSOPT based on the EMA-SCM. By construction, the SEPRIAL is 100 for the FSOPT and zero for the EMA-SCM. The average is taken over the 100 Monte-Carlo simulations. Our simulation experiments are organized around two aspects: convergence, and concentration ratio.

Since all EMA-SCM based estimators are parameterized by the exponential decay rate, we fix the hyperparameter β to be the same value for all experiments to ensure that the covariance estimators are comparable, and that any difference between the performances is due to the estimator’s ability to suppress the excess dispersion in the cross-sectional dimension. We also enforce that the characteristic time-scale T_e is not greater than the actual sample size T in the specifications for the simulated data.

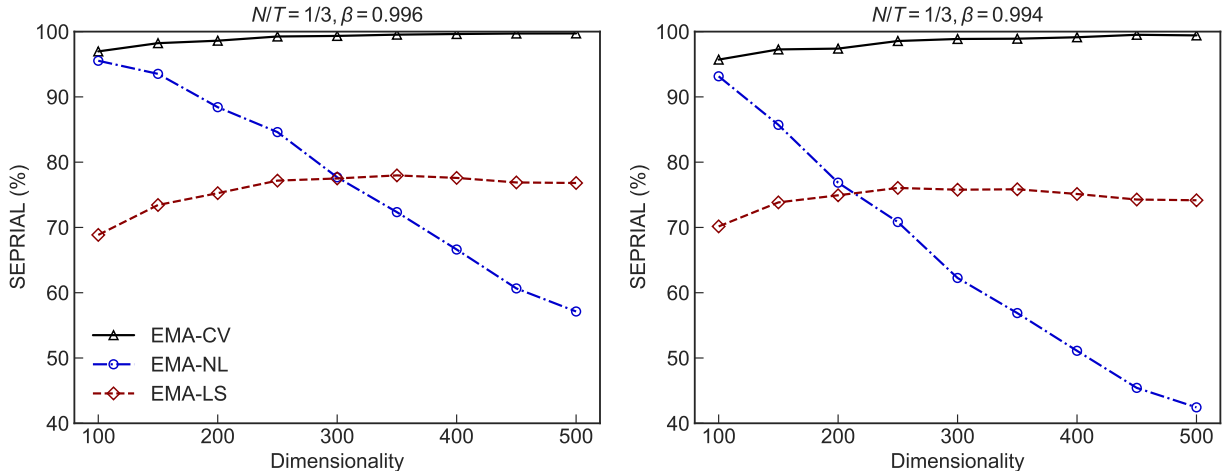


Figure 2: Convergence of the cross-validation, nonlinear and linear shrinkage estimators. The proportion of the eigenvalues set at values 1, 3 and 10 are distributed as 20%, 40% and 40%, respectively. The simulated data is normal random distributed and $N/T = 1/3$. Every point corresponds to an average over 100 repetitions.

4.2 Convergence

To analyze convergence, we allow both N and T to increase simultaneously while maintaining the concentration ratio N/T to be fixed at $1/3$. From the left panel of Figure 2, it can be seen that the EMA-CV estimator $\hat{\Sigma}$ performs well overall and with its SEPRIAL converging rapidly to 100% as the dimensionality of the matrix increases. The performance for EMA-LS, however, is suboptimal relative to EMA-CV, and remains stagnant in the high dimensional regime. This is because EMA-LS is constrained by its single global shrinkage intensity which limits its expressivity to capture the nonlinearities in the optimal shrinkage which posits different shrinkage intensities for different sample eigenvalues.

Note that the performance for the EMA-NL is comparable in the low dimensional regime but quickly deteriorates as the dimensionality of the matrix increases. In fact, the estimator starts to underperform relative to the EMA-LS past dimension 300. This is because, with increasing dimensionality, the presence of the null eigenvalues in the EMA-SCM becomes more prevalent which creates further distortion in the sample eigenvalues. This makes the task of inferring the correct shape of the distribution of population eigenvalues more challenging for EMA-NL which assumes that the noise in the sample eigenvalues are generated from an i.i.d. random matrix.

Plotting the estimated eigenvalues as a function of the sample eigenvalues for various covariance estimators, see Figure 3, sheds some light into this observation. The 45-degree line serves as a reference for which no adjustment to the sample eigenvalues were made; this corresponds to the identity function where the estimated eigenvalues are the sample eigenvalues themselves. The left panel of Figure 3 considers a typical simulation setting where N equals to a 100. We see that the EMA-LS linearly adjusts the sample eigenvalues by lifting small eigenvalues upwards and while pulling the large ones downwards towards their grand mean at 5.4. In contrast, EMA-CV shrinks both excessively large and small eigenvalues back towards the population values, avoiding null eigenvalues altogether. The shrinkage is non-linear in that different eigenvalues are shrunked by different amounts. EMA-NL behaves similar to EMA-CV, albeit there appears to be a slight downward (upward) bias in the small (large) eigenvalues.

In the higher dimensional setting where N equals to 500, we see a different response for EMA-CV and EMA-NL on the right panel of Figure 3. Implicitly, the effective concentration ratio q_e is now higher which can be seen to systematically inflate the noise in the sample eigenvalues. This information is internalized in EMA-CV which calls for a more intense shrinkage in the sample eigenvalues in order to reduce the cross-sectional dispersion that has been inflated by the time-dependent variance. In contrast, we see that

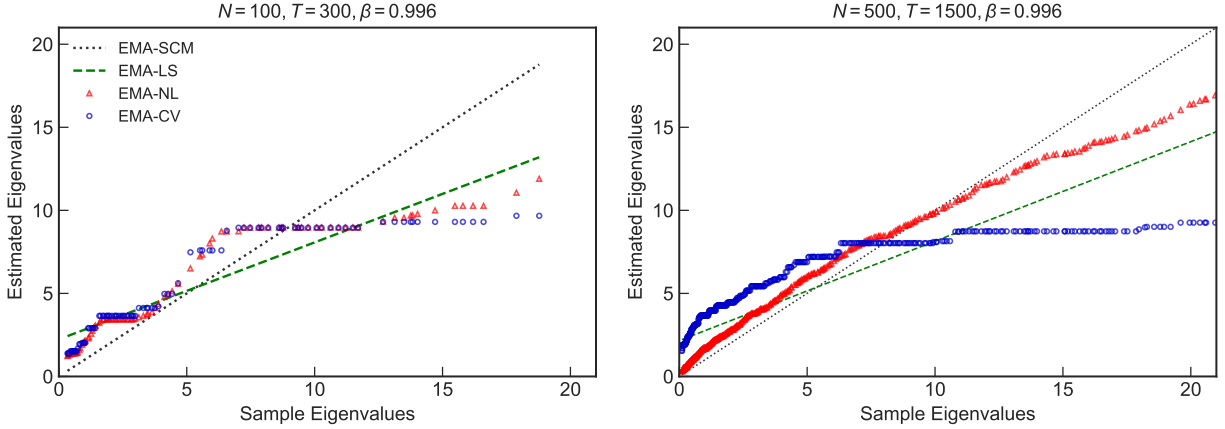


Figure 3: Responses of the cross-validation, nonlinear and linear shrinkage estimators. The proportion of the eigenvalues set at values 1, 3 and 10 are distributed as 20%, 40% and 40%, respectively. The simulated data is normal random distributed with $\beta = 0.996$ and $N = 100$ and $T = 300$ (left panel), and $N = 500$ and $T = 1500$ (right panel).

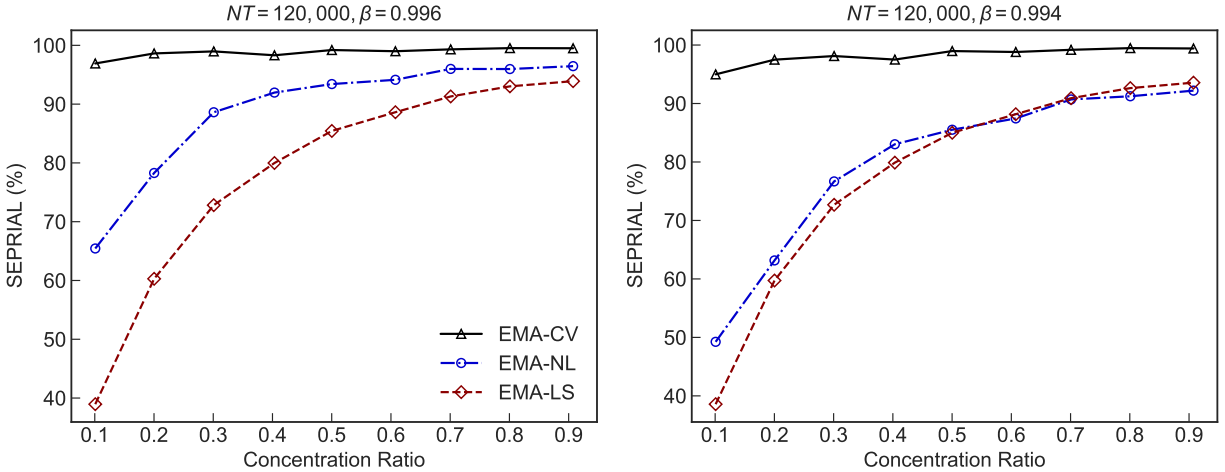


Figure 4: Effect of varying the concentration ratio N/T . The proportion of the eigenvalues set at values 1, 3 and 10 are distributed as 20%, 40% and 40%, respectively. The simulated data is normal random distributed with $\beta = 0.996$. Every point corresponds to an average over 100 repetitions.

EMA-NL nonlinearly shrinks the sample eigenvalues albeit not too aggressively.

Finally, the right panel of Figure 2 illustrates an identical setting with a lower decay rate β . Consequently, the exponential weights induce greater correlations in the recent observations and increase the effective concentration ratio for a fixed concentration ratio. We see that the performance for EMA-CV and EMA-LS remain robust to this change in regime except for EMA-NL which is now comparably worse across all dimensions. This is because, the shrinkage formula in Equation (5) for the EMA-NL hinges on the MP law (see Ledoit and Wolf, 2012) which is not capable to handle the excess dispersion induced by the weight correlations appropriately. In contrast, the EMA-CV estimator is “aware” of non-stationarity and adjusts the sample eigenvalues in a way that is consistent with an observation matrix of similar specification but with a sample size that is “effectively” smaller. For EMA-LS, however, the response is based on a shrinkage intensity that only depends on the concentration ratio, q which is held constant in this setting.

4.3 Concentration Ratio

We demonstrate how the SEPRIAL of the shrinkage estimators varies with the concentration ratio q if we maintain the product $N \times T$ fixed at 120,000. From Figure 4, we see that the EMA-CV estimator performs well for various configurations of the concentration ratio q while EMA-LS underperforms at low concentrations. This is because at low concentrations, the sample eigenvalues from the EMA-SCM can reveal information about their clustered and dispersed nature around the population eigenvalues. In this situation, a nonlinear shrinkage method can benefit from this information because it is flexible enough to shrink eigenvalues within clusters and with vanishing intensities between clusters. However, when the cross-sectional dimension is not negligible with respect to the sample size, this information becomes obscured by high-dimensional noise, which renders a simple linear approximation effective in higher concentrations.

Overall, the EMA-NL estimator performs moderately well for a decay rate at $\beta = 0.996$. There is an underperformance when the concentration is low, which is attributed to the fact that the adverse noise effects from weight induced correlations in the sample eigenvalues distort the information that is required for EMA-NL to optimally respond in shrinking the sample eigenvalues. The situation improves as the concentration ratio increases since the noise due to cross-sectional dispersion starts to overwhelm that from the time-dependent variance; EMA-NL is equipped to handle noise from the former than the latter. However, a noticeable wedge in the performance between EMA-CV and EMA-NL can be observed at all concentration ratios, whose size depends on the intensity of the exponential decay rate. Moreover, using a lower decay rate at $\beta = 0.994$ can be seen on the right panel of Figure 4 to systematically worsen the performance of EMA-NL and even change the ranking of the estimator at higher concentrations due to the further inflation of the adverse noise effects.

5 Empirical Analysis

5.1 Data and Portfolio Construction Rules

We obtain daily stock returns data from the Center for Research in Security Prices (CRSP), starting in 01/01/1981 and ending in 12/31/2019. Our analysis considers stocks from the NYSE, AMEX and NASDAQ stock exchanges. The size of the investment universe we consider is $N \in \{100, 200, 500, 1000\}$. We define one (trading) ‘month’ as 21 consecutive trading days. The portfolios that we construct are rebalanced on a monthly basis using a rolling window scheme where only past information is used to avoid a look-ahead bias. In particular, the covariance matrix is estimated using an in-sample period of size $T = 1250$ and evaluated using an out-of-sample test period of length $T_o = 21$. The out-of-sample period starts from 03/09/1986 to 31/12/2019. This provides us with a total of $m = 400$ months (or 8400 days) of consecutive, nonoverlapping observations with length 21 days for which the portfolios are rebalanced on.

To construct a well-defined investment universe which we can estimate the covariances on, we use a similar procedure described in Engle et al. (2019). For each rebalancing month $j = 0, 1, 2, \dots, m - 1$ (using a zero-based indexing), we first select the stocks that have complete data over in-sample period and out-of-sample test period. Then, we search for pairs of highly correlated stocks (that is, those with a sample correlation exceeding 0.95) and remove the stock with the lower volume in each pair.³ From this remaining set of stocks, we select the largest N stocks (as measured by their market capitalization on the rebalancing month m) to include in our investment universe.

Finally, we perform a normalization on each stock by its cross-sectional daily volatility period-by-period. A cross-sectional normalization removes variations in the scale of returns over time to create a comparable scale across stocks. This helps to correct the daily returns on periods with high volatility which prevents the portfolio from overweighting stocks with high volatility. We also ‘winsorize’ the data to obviate the possibility of outliers corrupting the covariance estimation.

³The identification and removal of highly correlated stocks can reduce the burden for portfolio optimizers since these pairs of stocks contribute little towards the benefit of diversification. The excess capacity in the fund’s budget constraint from this removal can then be deployed into other assets to reduce the overall portfolio risk.

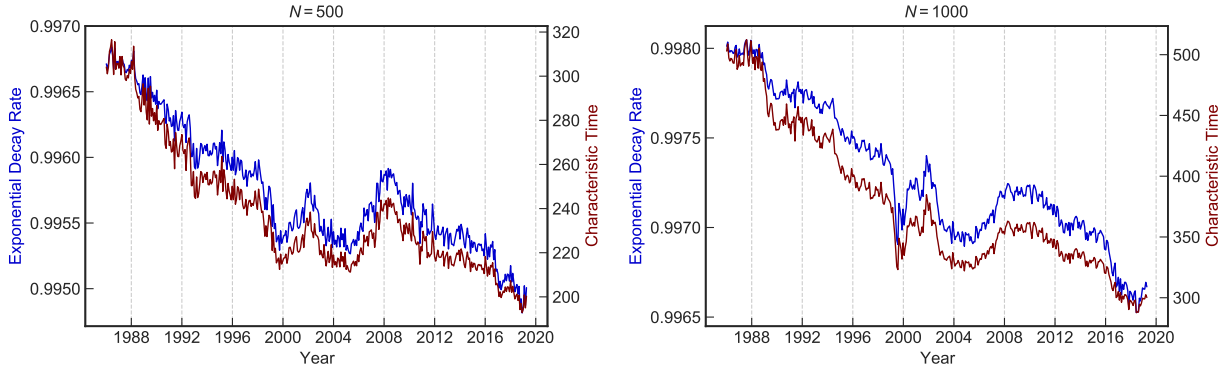


Figure 5: Evolution of the monthly-calibrated exponential decay rate and characteristic time-scale over the in-sample periods from 1981 to 2019. These quantities are estimated using a monthly rolling window of length $T = 1250$ with $N = 500$ stocks (left panel), $N = 1000$ stocks (right panel).

5.2 Hyperparameter Calibration

Given an investment universe, we can estimate the exponential decay rate, β by following the calibration procedure which we outlined in Section 3.5 using the rolling window scheme described in Section 5.1 to obtain their monthly values. We will use these calibrated quantities obtained from the investment universe of size $N \in \{100, 200, 500, 1000\}$ in the ensuing sections for the portfolio construction. Figure 5 shows the monthly evolution for the calibrated values of the exponential decay parameter $\hat{\beta}$ and its associated characteristic time-scale \hat{T}_e using $N = 500$ (left panel) and $N = 1000$ (right panel) assets with a estimation time window of length $T = 1250$.

The evolution of the memory decay parameter suggests that it is not a static quantity, but rather, it is time-varying in nature. We see that both calibrated quantities $\hat{\beta}$ and \hat{T}_e exhibit a declining trend from 1986 to 2019; this highlights that non-stationary effects have intensified in the later years, calling for a shorter time-scale to capture the risk profile of the set of liquid stocks from those periods. Moreover, the random fluctuations in the hyperparameter for $N = 1000$ are more compressed than that for $N = 500$ indicates that larger dimensional systems contribute towards the stability and regularity of the shape of the bulk spectrum from period to period.

One salient feature that one can observe is that the calibrated decay rates are close to one and become more pronounced with $N = 1000$ even though their value fluctuates over time. For high-dimensional systems, this is a desirable because a high memory decay helps to further smooth out the day-to-day noisy variations coming from a wide range of heterogeneous asset returns. By contrast, the RiskMetrics1994 methodology from J.P. Morgan/Reuters (1996) recommends a decay rate of $\beta = 0.94$ which we find is too low of a value for the investment universe sizes under our consideration. Indeed, a low memory decay increases the presence of very small or null eigenvalues which can deteriorate the conditioning property of the covariance matrix.

From risk management perspective, the small or null eigenvalues correspond to portfolios (or eigendirections) of little to zero risk. But this pathological example is a manifestation of the fact that there are insufficient samples relative to the number of assets to accurately characterize the risk landscape of the assets. A consequence of having a low memory decay relative to the number of assets is that the eigendirections corresponding the small eigenvalues can be seemingly suppressed in-sample; however, it is possible that variations in stock returns can materialize along these suppressed eigendirections giving rise to higher out-of-sample risk. As a result, the covariance matrix will tend to react more to recent shocks to return cross-products suboptimally and the portfolio can incur undue transaction costs. Thus, increasing the memory decay helps to mitigate this problem by introducing historical sources of randomness in the cross-section of asset returns.

5.3 Global Minimum Variance Portfolio

To test the performance of different covariance matrix estimators in the context of portfolio optimization, we assume that expected returns for all assets are identical and focus on the global minimum variance (GMV) portfolio which is the solution to the problem

$$\mathbf{w}^* = \arg \min_{\mathbf{w} \in \mathbb{R}^N} \mathbf{w}' \mathbf{C} \mathbf{w},$$

where $\mathbf{w} = (w_1, \dots, w_N)'$ is a vector of portfolio weights. This portfolio allocation framework is useful for isolating the estimation error stemming from the expected returns and allow us to focus solely on evaluating the quality of a covariance matrix estimator. Empirical studies of [Haugen and Baker \(1991\)](#) and [Jagannathan and Ma \(2003\)](#), among others, have found that the GMV portfolios enjoy favorable out-of-sample performance both in terms of risk and information ratio when compared with other benchmark portfolios.

Further constraints to the portfolio weights can be added into the optimization problem but it can diminish the effect of the covariance estimate since it reduces the set of feasible portfolios; (see [Jagannathan and Ma, 2003](#)). Hence, to allow for more detectable difference in the performance of portfolios obtained from various covariance estimation methods, we do not insist on any short-sales or magnitude constraint on the weights; the only constraint we require is the budget constraint where the portfolio weights sum to one to avoid the trivial solution where $\mathbf{w}^* = \mathbf{0}$. In this setting, the solution for optimal weights has an explicit form given by

$$\mathbf{w}^* = \frac{\mathbf{C}^{-1} \mathbf{1}}{\mathbf{1}' \mathbf{C}^{-1} \mathbf{1}}, \quad (14)$$

where $\mathbf{1}$ is an N -dimensional vector of ones. By replacing \mathbf{C} with an estimator of the population covariance matrix $\hat{\Sigma}$ yields a portfolio $\hat{\mathbf{w}}$ that can be computed from the returns data.

To evaluate the performance of the GMV portfolio, we compute three out-of-sample performance measures. Let $\tau_j = T + j \times T_o + 1$ index the first day in the out-of-sample period for a given (zero-based index) month $j \in \{0, \dots, m-1\}$. The quantities that we are interested in are:

- AV: Annualized average of the out-of-sample log returns \mathbf{r}_τ given by $AV = 252\hat{\mu}$, where

$$\hat{\mu} = \frac{1}{mT_o} \sum_{j=0}^{m-1} \sum_{\tau=\tau_j}^{\tau_j+T_o-1} \mathbf{w}' \mathbf{r}_\tau.$$

- SD: Annualized standard deviation of out-of-sample log returns \mathbf{r}_τ given by $SD = \sqrt{252}\hat{\sigma}$, where

$$\hat{\sigma} = \sqrt{\frac{1}{mT_o - 1} \sum_{j=0}^{m-1} \sum_{\tau=\tau_j}^{\tau_j+T_o-1} \left(\mathbf{w}' \mathbf{r}_\tau - \frac{\hat{\mu}}{252} \right)^2}.$$

- IR: Annualized information ratio given by the ratio AV/SD .

The primary metric for which we evaluate the performance of the GMV portfolio will be the out-of-sample standard deviation. Having a high portfolio average return and information ratio is beneficial but is of secondary importance to the objective of the GMV portfolio, which is to minimize the portfolio's variance.

5.4 List of Candidate Estimators

Given the plethora of covariance estimators in the literature, we limit ourselves to a few representative estimators. In particular, we consider the following portfolios in our study:

- **1/N**: the equal-weighted portfolio of [DeMiguel et al. \(2009\)](#).
- **EMA**: the GMV portfolio (14), where the estimator $\hat{\Sigma}(\hat{\mathbf{E}}; \beta)$ is the EMA-SCM itself.

- **EMA-LS**: the GMV portfolio (14), where the estimator $\hat{\Sigma}(\hat{\mathbf{E}}; \beta)$ is obtained from post-processing the EMA-SCM with the linear shrinkage of Ledoit and Wolf (2004b).
- **EMA-NL**: the GMV portfolio (14), where the estimator $\hat{\Sigma}(\hat{\mathbf{E}}; \beta)$ is obtained from post-processing the EMA-SCM with the non-linear shrinkage of Ledoit and Wolf (2020).
- **EMA-CV**: the GMV portfolio (14), where the estimator $\hat{\Sigma}(\hat{\mathbf{E}}; \beta)$ is obtained from post-processing the EMA-SCM with our proposed EMA-CV estimator described in Section 3.4.
- **SCM**: the GMV portfolio (14), where the estimator $\hat{\Sigma}(\hat{\mathbf{S}})$ is the SCM itself.
- **SCM-LS**: the GMV portfolio (14), where the estimator $\hat{\Sigma}(\hat{\mathbf{S}})$ is obtained from post-processing the SCM with the linear shrinkage of Ledoit and Wolf (2004b).
- **SCM-NL**: the GMV portfolio (14), where the estimator $\hat{\Sigma}(\hat{\mathbf{S}})$ is obtained from post-processing the SCM with non-linear shrinkage of Ledoit and Wolf (2020).
- **SCM-CV**: the GMV portfolio (14), where the estimator $\hat{\Sigma}(\hat{\mathbf{S}})$ is obtained from post-processing the SCM with the cross-validation of Bartz (2016).

Note that the progression from SCM-based portfolios to EMA-based portfolios, implies a departure from the rotation equivariance framework centered around the standard SCM. The reason is because the sample eigenvectors from the SCM are different from those of the EMA-SCM; the latter are based on a modified covariance matrix $\tilde{\mathbf{X}}'\tilde{\mathbf{X}}/T$ which reweighs the data points such that recent observations receive a greater weight than older observations. In effect, this amounts to making an *a priori* belief about the orientation of the population eigenvectors which is the non-stationarity in financial returns. As such, the following portfolio simulations demonstrates whether the incorporation such prior knowledge can be beneficial towards reducing the out-of-sample portfolio risk.

5.5 Portfolio Simulation Results

We report the performances for the various portfolios in Table 1, for the various estimation schemes, while maintaining the same value of T (the in-sample period) and T_o (the out-of-sample period). Since EMA-based portfolios are parameterized by β , we consider using their monthly calibrated values $\hat{\beta}$ from Section 5.2 in this experiment.

We summarize the out-of-sample results in Table 1 as follows:

- The $1/N$ portfolio is consistently outperformed by all other portfolios by a significant margin. The second-worst portfolio is the EMA portfolio;
- Among the EMA portfolios, there appears to be a ranking across all portfolio sizes N : EMA-CV, EMA-NL, EMA-LS, EMA. We will investigate the consistency of this ranking through the robustness checks in the following subsection;
- Among the SCM portfolios, the SCM performs the worst followed by SCM-LS. Both the SCM-NL and SCM-CV portfolios perform the best in this eigenbasis and remarkably share almost identical performance on all three measures;
- Interestingly, SCM-based portfolios can outperform some the EMA-based portfolios with the exception of EMA-CV. The setting where SCM-NL and SCM-CV portfolios underperform relative to the EMA-NL portfolio is with an investment universe of size $N = 1000$. This coincides with a relatively high calibrated memory decay used in the EMA-NL portfolio as seen in the right panel of Figure 5;
- Overall, the EMA-CV portfolio consistently delivers best result, owing, in part, to the non-stationary structure of the financial returns. The performance of this portfolio can also be seen to improve with the size of the investment universe N .

	1/ N	EMA	EMA-LS	EMA-NL	EMA-CV	SCM	SCM-LS	SCM-NL	SCM-CV
$N = 100$									
AV (%)	7.38	6.00	6.20	6.21	7.42	7.77	7.75	7.44	7.42
SD (%)	18.16	13.07	12.86	12.70	12.04	12.46	12.45	12.32	12.32
IR	0.41	0.45	0.48	0.49	0.62	0.62	0.62	0.60	0.60
$N = 200$									
AV (%)	7.37	9.60	9.52	9.38	8.84	9.47	9.47	8.97	8.95
SD (%)	17.94	12.33	11.94	11.46	10.60	11.39	11.34	11.08	11.08
IR	0.41	0.78	0.80	0.82	0.83	0.83	0.84	0.80	0.81
$N = 500$									
AV (%)	6.87	9.59	9.45	9.24	8.80	8.50	8.81	8.66	8.67
SD (%)	17.86	11.40	10.32	9.27	8.58	9.97	9.67	9.06	9.07
IR	0.38	0.84	0.92	1.00	1.03	0.85	0.91	0.96	0.96
$N = 1000$									
AV (%)	6.04	8.05	7.89	8.66	8.94	7.12	8.48	8.54	8.57
SD (%)	18.03	14.00	9.54	7.81	7.53	13.10	9.67	7.85	7.87
IR	0.33	0.57	0.83	1.11	1.19	0.54	0.88	1.08	1.08

Table 1: A summary of the annualized out-of-sample average log returns (AV), standard deviation of log returns (SD) and information ratio (IR) for each combination of investment universe size, N and covariance matrix estimator. The daily out-of-sample returns starts from 03/09/1986 and ends in 31/12/2019. All EMA-based portfolios are rebalanced each month using an estimation window of size $T = 1250$ and with a memory decay that has been calibrated to the in-sample observations. The most competitive SD value is highlighted in **bold**.

5.6 Robustness Check: Sensitivity Analysis

To perform a robustness check of our results, we first conduct a sensitivity analysis for the performance of the GMV portfolios based on different fixed values for β over the full sample period, see Figure 6. The reason for this exercise is threefold. First, the decay rate is often chosen to be a fixed quantity in practice. Second, it allows us to analyze how the EMA-based portfolios react to changes in the memory decay. Third, to determine if we can achieve a better result by simply using a fixed memory decay instead of using the memory-calibrated values. For all experiments in this section, we restrict the investment universe to be of size $N = 500$.

Additionally, we include annualized risk of the memory-calibrated portfolio for EMA-CV which is depicted as the horizontal red dashed line in Figure 6. This serves a visual reference for the other EMA-based portfolios which uses the same fixed memory decay over all estimation periods. The other memory-calibrated portfolios for EMA, EMA-LS and EMA-NL are excluded from the analysis since we do not see the same gains realized from these estimators that only uses a fixed memory decay. For example, in contrast to the results in Table 1, it is optimal for EMA and EMA-NL to pick a β close to or at 0.999, while EMA-LS seem to benefit from a much lower decay rate than what our calibration procedure prescribes in the right panel of Figure 5.

From Figure 6, EMA-CV shows that it can achieve the lowest annualized risk compared to the other

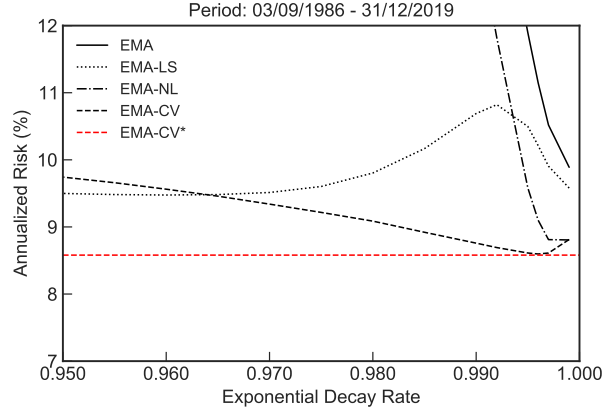


Figure 6: Annualized out-of-sample volatility of EMA-based portfolios with varying exponential decay rate evaluated on the full sample period from 03/09/1981 to 31/12/2019. The horizontal red dashed line corresponds to the out-of-sample volatility for the memory-calibrated EMA-CV portfolio.

estimators for an appropriately chosen fixed decay rate, β . Furthermore, the observation that the annualized risk can be further minimized for lower values of β indicate the presence of non-stationarity. Alternatively, we can arrive at a similar performance result for the minimum out-of-sample risk by using the calibrated values for the memory decay as seen in the horizontal red-dashed line in Figure 6. This approach uses only in-sample observations without relying on out-of-sample observations.

We see that EMA-NL can be competitive when the decay rate is chosen to be a value close to or at 0.999. However, both EMA and EMA-NL quickly underperform at an accelerated rate when the decay rate decreases. This sensitivity to changes in the memory decay specification may not be a desirable property since this limits the estimator’s ability to react quickly to current market conditions. Thus, this is the reason to believe that the competitive results for EMA-NL in Table 1 may not hold under more intensified non-stationary regimes. By contrast, EMA-CV and EMA-LS show that they are more robust towards perturbations in the memory decay.

Additionally, the ranking of the performances can change for a low enough memory decay with EMA-LS outperforming the other estimators. This is due to the fact that at lower decay factors, the information in the EMA-SCM becomes severely distorted by the non-stationary noise which makes it difficult for EMA-CV to precisely extract the true eigenvalues. In such non-stationary regime, linear shrinkage towards the identity matrix may be sufficient as the isotropic noise from the identity helps to establish a minimal level of variability that could occur along certain eigendirections in order to maintain stability in the portfolio’s performance.

5.7 Robustness Check: Subperiod Analysis

In addition to the previous analysis, we also perform a similar exercise in Figure 7 but by considering two distinct out-of-sample subperiods: 03/09/1986 to 19/06/1997 (first subperiod); and 27/02/2009 to 31/12/2019 (second subperiod). This enable us to check if the outperformance of EMA-CV in Table 1 is influenced by peculiar subperiod effects.

The subperiod analysis in Figure 7 illustrates that the outperformance of the memory-calibrated EMA-CV portfolio is consistent over time. Moreover, note that the value of the fixed decay rate corresponding to the minimum risk for the EMA-CV portfolio takes on the value $\beta = 0.997$ in the first subperiod and $\beta = 0.995$ in the second. This can be seen to be roughly in agreement with the calibrated values of $\hat{\beta}$ over these two subperiods; see right panel of Figure 5. While our calibration procedure which we outlined in Section 3.5 is not designed to minimize portfolio risk, this observation helps to lend credence to the validity of our proposed hyperparameter selection.

Interestingly, we observe that the overall level of portfolio risk is increased for all EMA-based portfolios in

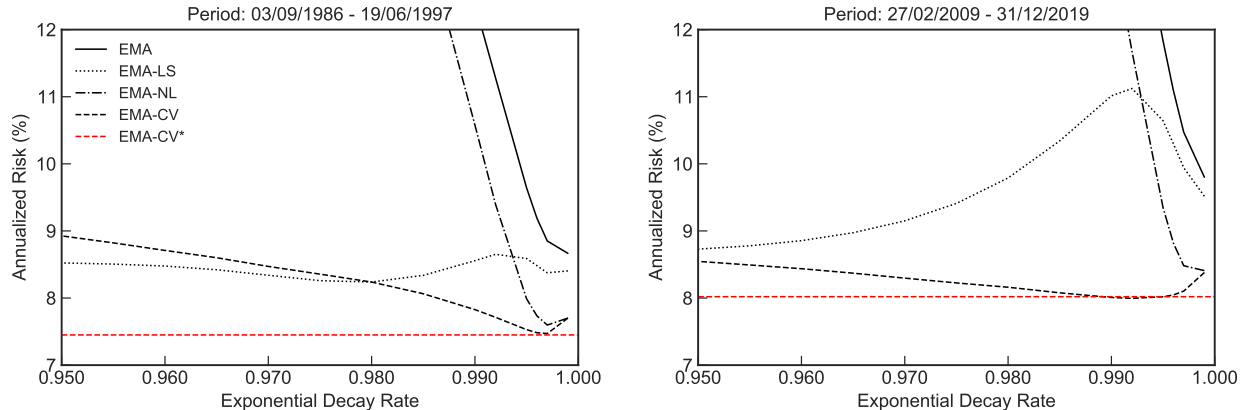


Figure 7: Annualized out-of-sample volatility of the EMA-based portfolios with varying exponential decay rate evaluated on two distinct subperiods: 03/09/1986 to 19/06/1997 (left panel) and 27/02/2009 to 31/12/2019 (right panel). The horizontal red dashed line corresponds to the out-of-sample volatility for the memory-calibrated EMA-CV portfolio obtained using the calibrated values for the memory decay.

the second subperiod than the first. This heightened level of risk coincides with a lower optimal fixed value of memory that minimizes the risk for the EMA-CV portfolio as seen in Figure 7. These differing values of the optimal memory decay is also supported by examining the level memory-calibrated values in these two subperiods in Figure 5. Thus, this observation suggests that the degree of non-stationarity as implied by the calibrated memory decay from a large system of assets can be predictive of the future performances of the portfolio risk.

6 Conclusion

This paper introduces a covariance estimator that seeks to attenuate the adverse noise effects that arise from both the cross-sectional and time-series dimensions in exponential moving average sample covariance matrices (EMA-SCM). The former requires us to extend the cross-validation shrinkage estimator of [Bartz \(2016\)](#) to handle the high-dimensional noise of weighted covariance matrices. The latter overcomes non-stationary noise by anchoring the theoretical spectra of an EMA-SCM to the data through the memory decay; the decay factor is tuned in such a way that it sufficiently describes the historical sources of randomness of the assets under consideration, using only in-sample observations. We find that the calibrated memory decay parameter exhibits a non-trivial time-varying behavior that scales with the cross-sectional dimension. Our simulation experiments help to reinforce the effectiveness of our estimator in shrinking the cross-sectional dispersion that has been further amplified by the time-dependent variance. Additionally, our backtest experiments on real financial data establishes that EMA-CV yields state-of-the-art performance when benchmarked against comparable estimators within the class of rotational equivariance.

In general, the adverse noise effects from a high-dimensional regime can be further reduced by incorporating additional prior knowledge about the orientation of the eigenvectors. For example, this can include overlaying the covariance matrix with economically driven models that possess a small number of risk parameters or with an appropriately structured block matrix reflecting the sector relationships of the stock returns. A cross-pollination of a postulated covariance matrix with the technology of non-linear shrinkage as employed in EMA-CV provides an avenue for further research. In addition, it was observed by [Jagannathan and Ma \(2003\)](#) that statistical shrinkage methods have a similar effect to imposing portfolio weight constraints that many mean-variance optimizers offer. Thus, it would be interesting to explore, through the analysis of [Zhao et al. \(2020\)](#), how the EMA-CV estimator interplays with leverage constraints in the high-dimensional setting in improving the portfolio's performance.

A Appendix

A.1 Spectral density and the Stieltjes transform

The *sample spectral density* of a $N \times N$ symmetric matrix \mathbf{E} is defined as,

$$\hat{\rho}_N(\lambda) := \frac{1}{N} \sum_{i=1}^N \delta(\lambda - \lambda_i), \quad (15)$$

where $\lambda_i, i = 1, 2, \dots, N$ are the sample eigenvalues of \mathbf{E} . The *limiting spectral density* (LSD), denoted as $\rho_{\mathbf{E}}(\lambda)$, is defined as the limit of (15) as $N \rightarrow \infty$, if it exists.

Since it is not easy to compute the LSD directly, we make use of the Stieltjes transform of a random matrix \mathbf{E} with $G : \mathbb{C} \setminus \mathbb{R} \rightarrow \mathbb{C}$ defined through the following integral relation

$$G(z) := \int_{\mathbb{R}} \frac{\rho(t)}{z - t} dt.$$

By construction, $G(z)$ computes the average of the trace of the resolvent $(\mathbf{E} - z\mathbb{I}_N)^{-1}$ in the high-dimensional limit

$$G(z) = \lim_{N \rightarrow \infty} -\frac{1}{N} \mathbb{E}[\text{Tr}(\mathbf{E} - z\mathbb{I}_N)^{-1}].$$

The Stieltjes transform encodes all the information about the density of eigenvalues. Such an encoding, however, is only useful if it is invertible as this provides a one-to-one mapping between probability densities on the real line and holomorphic functions in the upper half plane. Thus, to access the LSD, one has to compute the resolvent for the random matrix \mathbf{E} and invert its integral relation using the following inversion formula

$$\rho(\lambda) = -\frac{1}{\pi} \lim_{\eta \rightarrow 0^+} \text{Im } G^+(\lambda + i\eta),$$

where $G^+(z) := G(\lambda + i\eta)$ is the Stieltjes transform located above the branch cut. In particular, the eigenvalues are determined from the singularities of $G(z)$ on the real line.

A.2 Additive Free Probability Review

Given two matrices \mathbf{A} and \mathbf{B} , we would like to know the spectrum of $\mathbf{A} + \mathbf{B}$. In general, the spectrum of $\mathbf{A} + \mathbf{B}$ does not only depend on the spectrum of \mathbf{A} and \mathbf{B} ; one also needs to know the relative positions of the eigenvectors of \mathbf{A} and \mathbf{B} . However, in the high-dimensional asymptotic setting, free probability allows us to analyze the case where \mathbf{A} and \mathbf{B} are statistically independent, and the eigenvectors are in “generic positions” (Speicher, 2011); that is, the orientation of the eigenbases are as random as possible with respect to each others. In particular, two matrices \mathbf{A} and \mathbf{B} are said to be freely independent if

$$\mathbb{E}[f_1(\mathbf{A})g_1(\mathbf{B}) \dots f_k(\mathbf{A})g_k(\mathbf{B})] = 0,$$

such that $\mathbb{E}[f_i(\mathbf{A})] = 0$, and $\mathbb{E}[g_i(\mathbf{B})] = 0$ for any function f_i and g_i with $i = 1, 2, \dots, k$. Since $k = 1$ corresponds to classical independence, we see that the notion of freeness generalizes the concept of independence between random variables for non-commutative objects.

If the two matrices \mathbf{A} and \mathbf{B} are freely independent, then we can recover the spectrum of the sum $\mathbf{A} + \mathbf{B}$ from the spectrum of the individual matrices using an auxiliary object known as the R -transform. Given the Stieltjes transform G of a probability distribution ρ , the R -transform is defined as the solution to the functional equation

$$R(G(z)) + \frac{1}{G(z)} = z. \quad (16)$$

Consider the Blue function introduced by Zee (1996) which is defined as the functional inverse of $G(z)$ through the following relationship, $B(G(z)) = G(B(z)) = z$. If we let $w \equiv G(z)$, then Equation (16) reads,

$$R(w) = B(w) - \frac{1}{w}.$$

The advantage of the R -transform is that it linearizes the free additive convolution, in the sense that,

$$R_{\mathbf{A}+\mathbf{B}} = R_{\mathbf{A}} + R_{\mathbf{B}}.$$

Thus, the R -transform can be seen as the free analogue of the log of the Fourier transform.

We can summarize the derivation of the spectrum of $\mathbf{A} + \mathbf{B}$ as follows: 1) Compute the Stieltjes transforms $G_{\mathbf{A}}$ and $G_{\mathbf{B}}$ of $\rho_{\mathbf{A}}$ and $\rho_{\mathbf{B}}$; 2) Compute the R -transforms $R_{\mathbf{A}}$ and $R_{\mathbf{B}}$ from $G_{\mathbf{A}}$ and $G_{\mathbf{B}}$; 3) Compute the Stieltjes transform $G_{\mathbf{A}+\mathbf{B}}$ from $R_{\mathbf{A}+\mathbf{B}} = R_{\mathbf{A}} + R_{\mathbf{B}}$; 4) Invert the Stieltjes transform $G_{\mathbf{A}+\mathbf{B}}$ using to inversion formula to obtain $\rho_{\mathbf{A}+\mathbf{B}}$.

A.3 Computation of the Limiting Spectral Density and its Support

We are interested to analytically obtain the LSD $\rho_{\mathbf{E}}$ for the EMA-SCM. To this end, we write the EMA-SCM with time-scale T_e as

$$\hat{\mathbf{E}}_N(\tau, T) = \frac{1}{N} \sum_{t=1}^T b_N(t) \mathbf{x}_{\tau-t-1} \mathbf{x}'_{\tau-t-1} \equiv \frac{1}{N} \sum_{t=1}^T \mathbf{H}_t, \quad (17)$$

where $\mathbf{H}_t := b_N(t) \mathbf{x}_{\tau-t-1} \mathbf{x}'_{\tau-t-1}$ are rank-one matrices with $N - 1$ zero eigenvalues. The weight profiles can be expressed in terms of its effective concentration ratio q_e given by

$$b_N(t) := N \frac{1 - \beta}{1 - \beta^T} \beta^{t-1} = \frac{q_e}{1 - (1 - q_e/N)^T} \left(1 - \frac{q_e}{N}\right)^{t-1}, \quad \text{for } t = 1, 2, \dots, T.$$

We operate under the assumption that the matrix \mathbf{X} is a matrix of i.i.d. standard normal random variables of dimension $T \times N$. As such, matrices \mathbf{H}_t for $t = 1, 2, \dots, T$ are both independent and rotationally invariant. This assumption allows $\mathbf{H}_1, \mathbf{H}_2, \dots, \mathbf{H}_T$ to be asymptotically free. Moreover, we see that \mathbf{H}_t has one non-zero eigenvalue equal to $N^{-1} b_N(t) \|\mathbf{x}_{\tau-t-1}\|^2$ which is approximately equal to $b_N(t)$ for large N by the law of large numbers.

Since the EMA-SCM is expressed as a sum of freely independent matrices, the R -transform of the EMA-SCM $\hat{\mathbf{E}}_N$ is given by

$$R_{\mathbf{E}_N}(z) = \sum_{t=1}^T R_t(z),$$

where $R_t(z)$ is the R -transform of \mathbf{H}_t for $t = 1, 2, \dots, T$. To determine $R_{\mathbf{E}_N}(z)$, we need to know the R -transforms of its constituent parts. We first calculate the Stieltjes transform of \mathbf{H}_t which is given by

$$G_t(z) \equiv \frac{1}{N} \text{Tr}(z \mathbb{I}_N - \mathbf{H}_t)^{-1} = \frac{1}{N} \frac{1}{z - b_N(t)} + \frac{N-1}{N} \frac{1}{z}.$$

Using the functional inverse relationship between the Stieltjes transform and the Blue function, we have

$$z = G_t(B_t(z)) = \frac{1}{N} \frac{1}{B_t(z) - b_N(t)} + \frac{N-1}{N} \frac{1}{B_t(z)}.$$

Solving the quadratic equation in $B_t(z)$ gives

$$B_t(z_{\pm}) = \frac{1}{2z} \left(b_N(t)z - 1 \pm (1 + b_N(t)z) \sqrt{1 - \frac{4b_N(t)z}{N(1 + b_N(t)z)^2}} \right).$$

The functional equation $z = B_t(G_t(z))$ has two solutions and so one has to be careful to choose the right one. Thus, one chooses the solution among the multiple roots that satisfies the decay condition $G_t(z) \sim 1/z$ as $z \rightarrow \infty$ and the requirement that $G_t(z)$ must be analytic off the real line (Tao, 2011). If we consider the solutions to first order in $1/N$, then

$$B_t(z) = \frac{1}{z} + \frac{b_N(t)}{N(1 - b_N(t)z)}.$$

The R -transform of \mathbf{H}_t can be easily calculated as

$$R_t(z) = B_t(z) - \frac{1}{z} = \frac{b_N(t)}{N(1 - b_N(t)z)}.$$

Free matrix addition gives us R -transform of \mathbf{E}_N

$$R_{\mathbf{E}_N}(z) = \frac{1}{N} \sum_{t=1}^T \frac{b_N(t)}{1 - b_N(t)z}.$$

In the high-dimensional asymptotic limit, we have

$$R_{\mathbf{E}}(z) = \int_0^{q^{-1}} \frac{\alpha \exp(-q_e x)}{1 - \alpha \exp(-q_e x)z} dx,$$

as $N, T \rightarrow \infty$ since

$$\lim_{N \rightarrow \infty} b_N(t) = \lim_{N \rightarrow \infty} \frac{q_e \sigma^2}{1 - (1 - q_e/N)^T} \left(1 - \frac{q_e}{N}\right)^t = \alpha \exp(-q_e x),$$

where $\alpha := q_e \sigma^2 (1 - \exp(-q_e/q))^{-1}$ for $x \in [0, q^{-1}]$. The integral in the $R_{\mathbf{E}}$ -transform can be evaluated to yield

$$R_{\mathbf{E}}(z) = \frac{\log(1 - \alpha \exp(-q_e/q)z)}{q_e z} - \frac{\log(1 - \alpha z)}{q_e z}.$$

Note that, in the limit $q_e \rightarrow 0$, we recover the R -transform of the Marčenko-Pastur spectrum

$$R_{\text{MP}}(z) = \frac{1}{1 - qz}.$$

The Blue function corresponding to the R -transform of the EMA-SCM is given by

$$B_{\mathbf{E}}(z) = R_{\mathbf{E}}(z) + \frac{1}{z} = \frac{1}{z} \left(1 - \frac{\log(1 - \alpha z)}{q_e} + \frac{\log(1 - \alpha \exp(-q_e/q)z)}{q_e}\right), \quad (18)$$

which is the exact expression found in Burda et al. (2011). Finally, using the functional equation $z = B_{\mathbf{E}}(G_{\mathbf{E}}(z))$, we arrive at the Stieltjes transform of the EMA-SCM which is given by⁴

$$G_{\mathbf{E}}(z) = - \left[z - \frac{1}{q_e} \log \left(\frac{1 - \alpha G_{\mathbf{E}}(z)}{1 - \alpha \exp(-q_e/q) G_{\mathbf{E}}(z)} \right) \right]^{-1}. \quad (19)$$

One can numerically solve for $G_{\mathbf{E}}(z)$ using the self-consistent equation in Equation (19) to arrive at the LSD $\rho_{\mathbf{E}}(\lambda; q, q_e)$ using the inversion formula.

⁴Note that $G_{\mathbf{E}}(z)$ is defined in the vicinity of $|z|$ large. However, by the analyticity of $G_{\mathbf{E}}(z)$, we can analytically continue it to the whole complex plane \mathbb{C}^+ ; this allows us to arrive at an analytic formula close to the real axis. Since $G_{\mathbf{E}}(z)$ introduces a branch-cut, we choose it such that $\text{Im}(G_{\mathbf{E}}(z)) > 0$ for $z \in \mathbb{C}^+$.

Finally, the upper and lower edges of the spectrum for which the support of the spectrum is defined on can be obtained by solving the following equation

$$\lambda_{\pm} = B_{\mathbf{E}}(z_{\pm}), \quad \text{where} \quad B'_{\mathbf{E}}(z_{\pm}) = 0.$$

To gain insight into the behavior of the lower edge of the spectrum, one can consider the case where $q \rightarrow 0$ as in [Bouchaud and Potters \(2009\)](#) and [Bouchaud et al. \(2005\)](#). Then the equation which characterizes the solution for the spectrum edges is given by

$$\lambda_{\pm} = \log(\lambda_{\pm}) + q_e + 1.$$

For $q_e \neq 0$, one can solve for λ_- to find that as the high-dimensional noise, N increases or the memory decay, β decreases, the lower edge tends exponentially fast to some value that is close to zero.

References

- Abadir, K. M., Distaso, W., and Žikeš, F. (2014). Design-Free Estimation of Variance Matrices. *Journal of Econometrics*, 181(2):165–180.
- Barlow, R. E., Brunk, H. D., Bartholomew, D. J., and Bremner, J. M. (1972). *Statistical Inference Under Order Restrictions: Theory and Application of Isotonic Regression*. Wiley, New York.
- Bartz, D. (2016). Cross-Validation Based Nonlinear Shrinkage. *arXiv preprint arXiv:1611.00798*.
- Bartz, D., Hatrick, K., Hesse, C. W., Müller, K.-R., and Lemm, S. (2011). Directional Variance Adjustment: Improving Covariance Estimates for High-Dimensional Portfolio Optimization. *arXiv preprint arXiv:1109.3069*.
- Bickel, P. J. and Levina, E. (2008). Covariance Regularization by Thresholding. *The Annals of Statistics*, 36(6):2577–2604.
- Bouchaud, J.-P. and Potters, M. (2009). Financial Applications of Random Matrix Theory: A Short Review. *arXiv preprint arXiv:0910.1205*.
- Bouchaud, J.-P. and Potters, M. (2020). A First Course in Random Matrix Theory: for Physicists, Engineers and Data Scientists. *Cambridge University Press*.
- Bouchaud, J.-P., Potters, M., and Laloux, L. (2005). Financial applications of random matrix theory: Old laces and new pieces. *arXiv preprint physics/0507111*.
- Bun, J., Bouchaud, J.-P., and Potters, M. (2017). Cleaning Large Correlation Matrices: Tools from Random Matrix Theory. *Physics Reports*, 666:1–109.
- Burda, Z., Jarosz, A., Nowak, M. A., Jurkiewicz, J., Papp, G., and Zahed, I. (2011). Applying Free Random Variables to Random Matrix Analysis of Financial Data. Part I: The Gaussian Case. *Quantitative Finance*, 11(7):1103–1124.
- Cont, R. (2001). Empirical Properties of Asset Returns: Stylized Facts and Statistical Issues. *Quantitative Finance*, 1(2):223–236.
- DeMiguel, V., Garlappi, L., and Uppal, R. (2009). Optimal Versus Naive Diversification: How Inefficient is the 1/n Portfolio Strategy? *The review of Financial studies*, 22(5):1915–1953.
- El Karoui, N. (2008). Spectrum Estimation for Large Dimensional Covariance Matrices Using Random Matrix Theory. *Annals of Statistics*, 36(6):2757–2790.
- Engle, R. F. (2002). Dynamic Conditional Correlation: A Simple Class of Multivariate Generalized Autoregressive Conditional Heteroskedasticity Models. *Journal of Business & Economic Statistics*, 20(3):339–350.
- Engle, R. F., Ledoit, O., and Wolf, M. (2019). Large Dynamic Covariance Matrices. *Journal of Business & Economic Statistics*, 37(2):363–375.
- Fan, J., Liao, Y., and Mincheva, M. (2012). Large Covariance Estimation by Thresholding Principal Orthogonal Complements. *Journal of the Royal Statistical Society. Series B, Statistical methodology*, 75(4).
- Haugen, R. A. and Baker, N. L. (1991). The Efficient Market Inefficiency of Capitalization-Weighted Stock Portfolios. *The Journal of Portfolio Management*, 17(3):35–40.
- Jagannathan, R. and Ma, T. (2003). Risk Reduction in Large Portfolios: Why Imposing the Wrong Constraints Helps. *The Journal of Finance*, 58(4):1651–1683.
- J.P. Morgan/Reuters (1996). RiskMetrics - Technical Document. *New York: J.P. Morgan/Reuters*.

- Lam, C. (2016). Nonparametric Eigenvalue-Regularized Precision or Covariance Matrix Estimator. *The Annals of Statistics*, 44(3):928–953.
- Ledoit, O. and Péché, S. (2011). Eigenvectors of Some Large Sample Covariance Matrix Ensembles. *Probability Theory and Related Fields*, 151(1-2):233–264.
- Ledoit, O. and Wolf, M. (2004a). Honey, I Shrunk the Sample Covariance Matrix. *Journal of Portfolio Management*, 30(4):110–119.
- Ledoit, O. and Wolf, M. (2004b). A Well-Conditioned Estimator for Large-dimensional Covariance Matrices. *Journal of multivariate analysis*, 88(2):365–411.
- Ledoit, O. and Wolf, M. (2012). Nonlinear Shrinkage Estimation of Large-Dimensional Covariance Matrices. *The Annals of Statistics*, 40(2):1024–1060.
- Ledoit, O. and Wolf, M. (2015). Spectrum Estimation: A Unified Framework for Covariance Matrix Estimation and PCA in Large Dimensions. *Journal of Multivariate Analysis*, 139(2):360–384.
- Ledoit, O. and Wolf, M. (2020). Analytical Nonlinear Shrinkage of Large-Dimensional Covariance Matrices. *The Annals of Statistics*, 48(5):3043–3065.
- Lettau, M. and Pelger, M. (2020). Factors That Fit the Time Series and Cross-Section of Stock Returns. *The Review of Financial Studies*, 33(5):2274–2325.
- Lin, J. (1991). Divergence Measures Based on the Shannon Entropy. *IEEE Transactions on Information theory*, 37(1):145–151.
- Marčenko, V. A. and Pastur, L. A. (1967). Distribution of Eigenvalues for Some Sets of Random Matrices. *Mathematics of the USSR-Sbornik*, 1(4):457.
- Pafka, S., Potters, M., and Kondor, I. (2004). Exponential Weighting and Random-Matrix-Theory-Based Filtering of Financial Covariance Matrices for Portfolio Optimization. *arXiv preprint cond-mat/0402573*.
- Rajaratnam, B., Massam, H., and Carvalho, C. M. (2008). Flexible Covariance Estimation in Graphical Gaussian Models. *The Annals of Statistics*, 36(6):2818–2849.
- Speicher, R. (2011). Free Probability Theory. In *The Oxford handbook of Random Matrix Theory*, page 452–470. Oxford University Press.
- Stein, C. (1975). Estimation of a Covariance Matrix. Rietz lecture, 39th Annual Meeting IMS. Atlanta, Georgia.
- Stein, C. (1986). Lectures on the Theory of Estimation of Many Parameters. *Journal of Mathematical Sciences*, 34(1):1373–1403.
- Tao, T. (2011). Topics in Random Matrix Theory. In *Graduate Studies in Mathematics*, volume 132, Providence, Rhode Island.
- Wigner, E. (1955). Characteristic Vectors of Bordered Matrices with Infinite Dimensions. *Annals of Mathematics*, 62:548–564.
- Zee, A. (1996). Law of Addition in Random Matrix Theory. *Nuclear Physics B*, 474(3):726–744.
- Zhao, Z., Ledoit, O., and Jiang, H. (2020). Risk Reduction and Efficiency Increase in Large Portfolios: Leverage and Shrinkage. *University of Zurich, Department of Economics, Working Paper*, (328).
- Zumbach, G. (2007). The RiskMetrics 2006 Methodology. *Technical Report, RiskMetrics Group*.